A double-lithography and double-reflow process and application to multi-pitch multi-height mechanical flexible interconnects

2017 J. Micromech. Microeng. 27 025014

(http://iopscience.iop.org/0960-1317/27/2/025014)

IOP Publishing

Journal of Micromechanics and Microengineering

J. Micromech. Microeng. **27** (2017) 025014 (6pp)

doi:10.1088/1361-6439/aa5401

A double-lithography and double-reflow process and application to multi-pitch multi-height mechanical flexible interconnects

Chaoqi Zhang, Hyung Suk Yang and Muhannad S Bakir

School of Electrical and Computer Engineering, Georgia Institute of Technology, Atlanta, GA 30332, USA

E-mail: chqzhang@gatech.edu and mbakir@ece.gatech.edu

Received 25 May 2016, revised 6 December 2016
Accepted for publication 15 December 2016
Published 11 January 2017

Abstract

Wafer-level multi-pitch and multi-height mechanically flexible interconnects (MPMH MFIs) are demonstrated using a double-lithography and double-reflow process of a large array of sacrificial polymer domes with various heights (ranging from 26 μm to 66 μm). Using these domes, NiW MFIs with various pitches (ranging from 50 μm to 150 μm) are formed atop the multi-height domes using electroplating. The mechanical and electrical properties of the fabricated MPMH MFIs are characterized using indentation and four-point resistance measurements.

Keywords: flexible interconnects, double-lithography, double-reflow, advanced packaging

(Some figures may appear in colour only in the online journal)

1. Introduction

Flexible interconnects have been widely investigated over the past two decades for chip reliability enhancement [1–5] and advanced probing [6, 7]. These previously reported flexible interconnects have a key common feature: the flexible interconnects are fabricated with an identical gap-height across the chip (or wafer), which makes them principally suitable for assembly on an initially relatively flat substrate to overcome the CTE mismatch and warpage during the bonding process or field use. However, there has been a great deal of recent efforts to develop advanced interposer based package and flip-chip assemblies [8]. Such applications, like the substrate stacking shown in figure 1, create the need for chip I/O interconnects with different gap-heights; in figure 1, the small gap-height and fine-pitch flexible interconnects are used to electrically connect assembled dice on the bottom substrate to a second stacked (top) substrate while the large gap-height flexible interconnects are used to directly interconnect the two substrates by traversing the assembled dice on the bottom substrate.

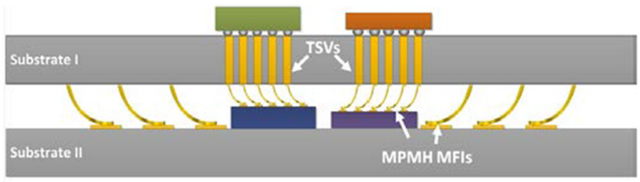

Figure 1. Assembly on a package with embedded chips using multi-pitch multi-height mechanically flexible interconnects (MPMH MFIs).

A brute-force approach to the fabrication of such a hybrid gap-height interconnect array could be achieved by fabricating the flexible interconnects with different heights and pitches sequentially. Due to the potential complexity of the process, the fabrication throughput and yield may suffer compared to the uniform gap-height array process reported in [9–13]. To address this need, we report a double-lithography and double-reflow process in this paper and apply it to the formation of multi-pitch multi-height mechanically flexible interconnects (MPMH MFIs). This process is based on our previously

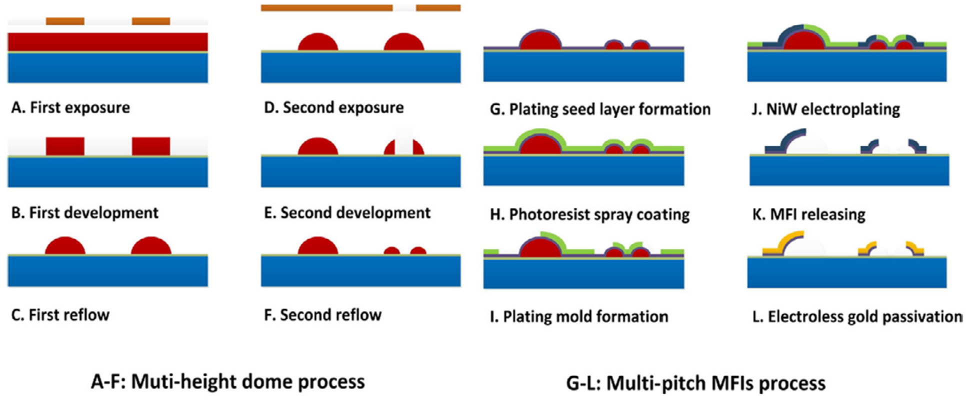

Figure 2. Fabrication of multi-pitch multi-height MFIs using double-lithography and double-reflow process. (A) First exposure, (B) first development, (C) first reflow, (D) second exposure, (E) second development, (F) second reflow, (G) plating seed layer formation, (H) photoresist spray coating, (I) plating mold formation, (J) NiW electroplating, (K) MFI releasing, (L) electroless gold passivation.

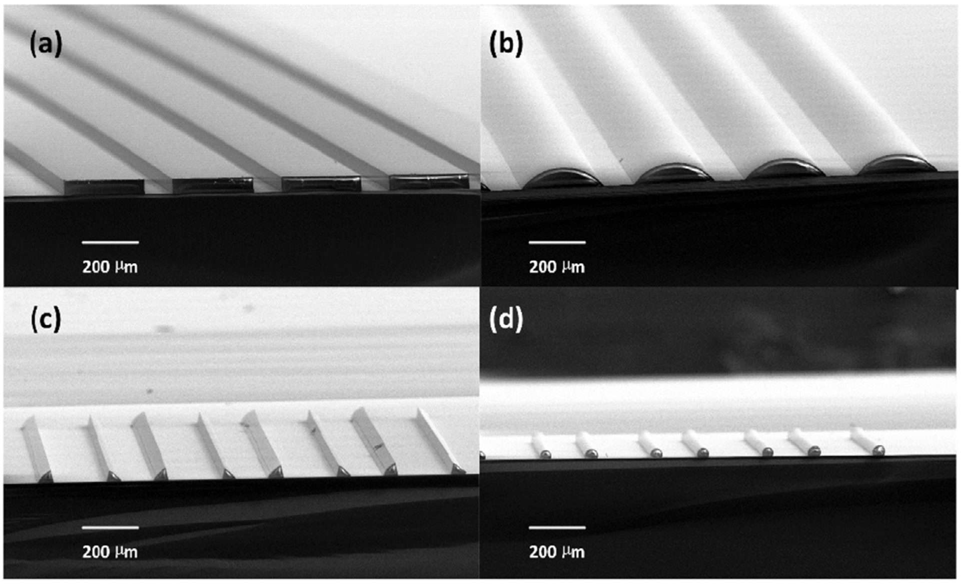

Figure 3. 2 Key steps of double-lithography and double-reflow: (a) polymer strips after first development; (b) polymer domes after first reflow; (c) polymer strips after second development and (d) polymer domes after second development.

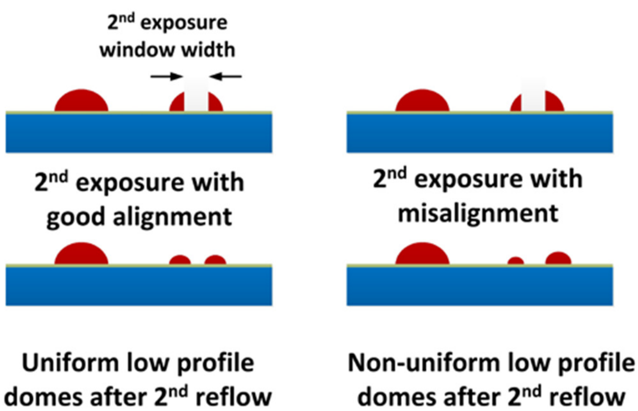

Figure 4. Non-uniform height domes resulting from the misalignment of second exposure.

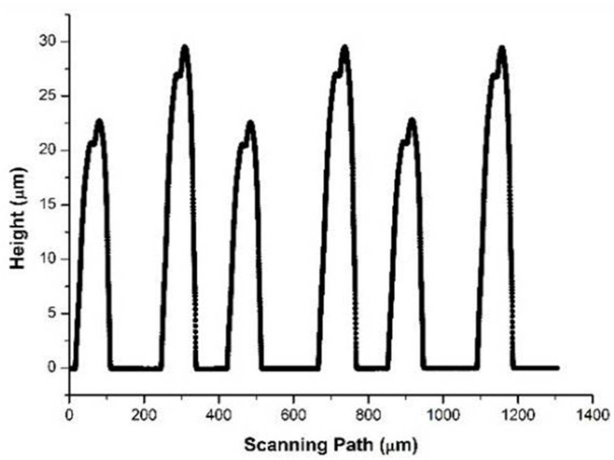

Figure 5. Dome height variation induced by second exposure misalignment.

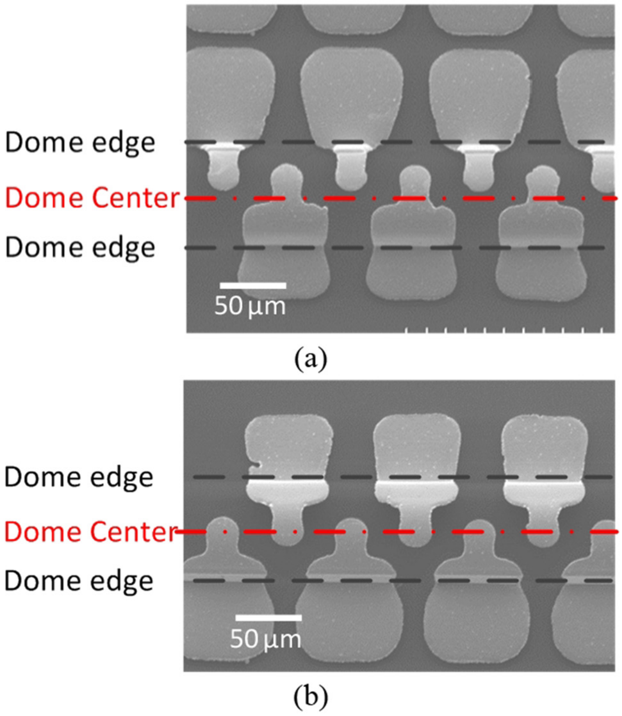

Figure 6. MFI geometry distortion induced by the misalignment of the second exposure: (a) MFIs formed on a dome with peak position shift induced by misalignment, and (b) MFIs formed on a dome without peak position shift after correct second exposure.

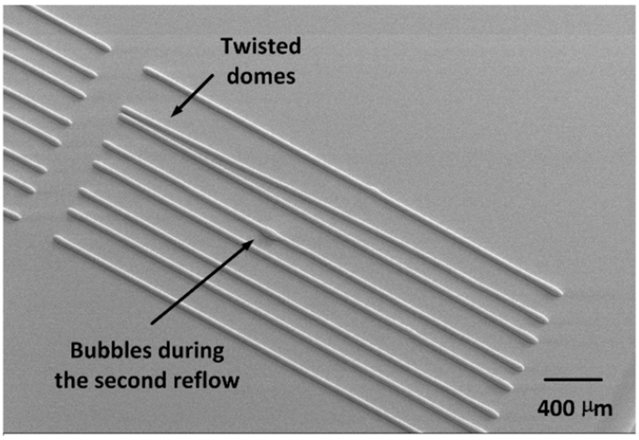

Figure 7. SEM image of: (a) dome twisting after second exposure, and (b) bubbles formation in photoresist during second reflow.

reported Au–NiW MFI technology [9–13]. The reported MFIs are promising for rematable interconnect applications, such as active wafer-level probing [14], large scale 2.5D interconnection [15–17], advanced thermal isolation [18].

This paper is organized as follows: section 1 describes the formation of domes with various heights (multi-height domes) using a double-lithography and double-reflow process. Next, in section 2, this paper reports multi-pitch MFIs formed above the multi-height domes. Mechanical and electrical experimental characterizations of the MPMH MFIs are reported in section 3. Finally, section 4 is the conclusion.

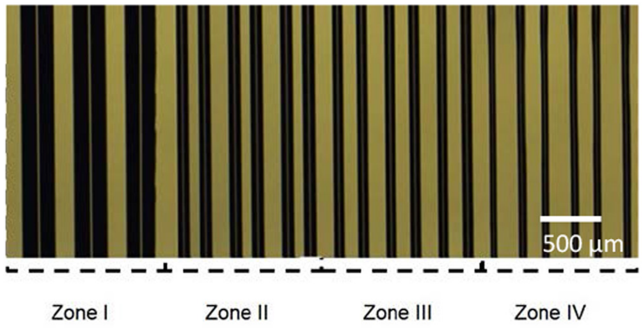

Figure 8. Multi-height domes after double-lithography and double-reflow process.

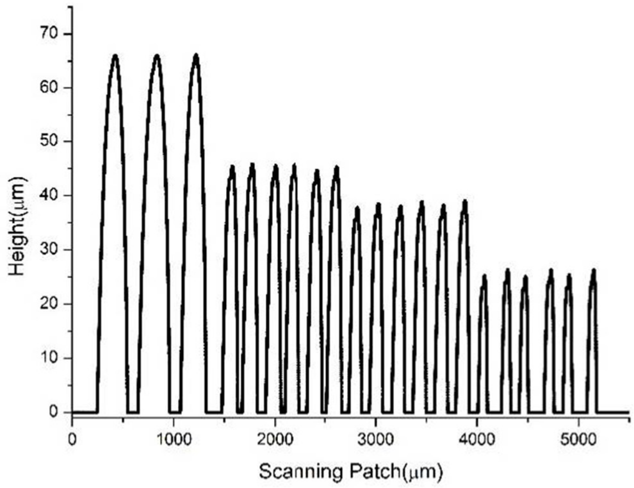

Figure 9. Muti-height dome profile.

2. Fabrication of multi-pitch multi-height MFIs

As shown in figure 2, the fabrication of MPMH MFIs consists of two major steps: multi-height dome and multi-pitch MFI fabrication. These processes are described in this section.

2.1. Fabrication of multi-height domes

The double-lithography and double-reflow process is shown in figure 2 steps (A)–(F). The process begins with the formation of large sacrificial polymer domes using the first mask exposure and thermal reflow process shown in figure 2 steps (A)–(C); note that this is the same process used to fabricate the previously reported uniform gap-height MFIs [9–11]. The 45 μm thick photoresist layer in step (B) is fabricated using multiple coatings of a thick positive photoresist. After reflow, the dome height is approximately 66 μm [11]. Moreover, note that the formed domes, which are fabricated using positive photoresist, are unexposed at this stage in the process. Thus, following a controlled first reflow step, the positive photoresist domes remain UV-light sensitive. Next, a second mask exposure (step (D) shown in figure 2) is performed on specific domes (i.e. the right dome in step (D) of figure 2); these will ultimately be the domes with smaller height.

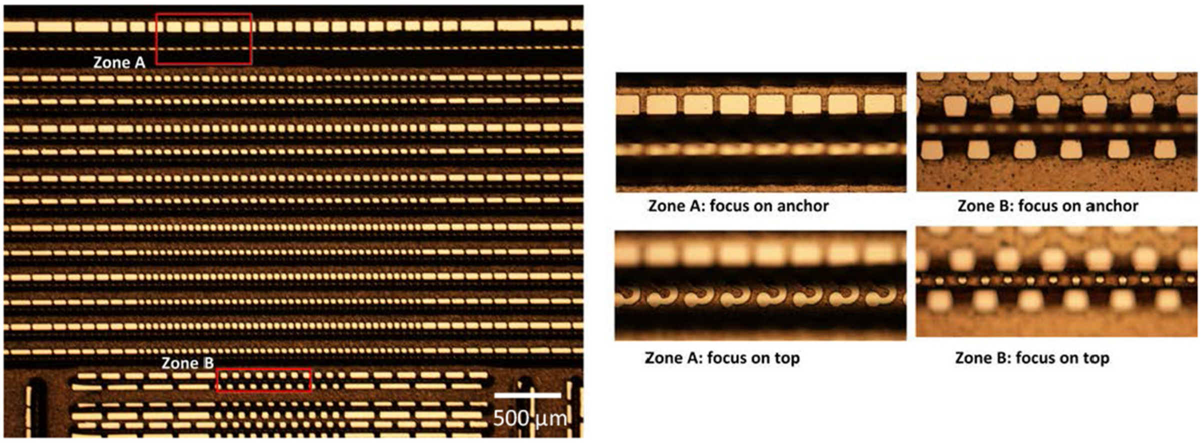

Figure 10. A photoresist electroplating mold with a large array-area pattern of multi-pitch MFIs. Resolved patterns are obtained for both the large-profile MFIs (Zone A) and the low-profile MFIs (Zone B).

Table 1. Multi-height dome dimensions.

Zone number	Dome width (μm)	Dome height (μm)	In-line pitch of MFIs on dome (μm)
I	300	150	66
II	100	80	45
III	75	60	38
IV	50	50	26

Following the second post-exposure development, only the edges of the corresponding original domes remain. During the second reflow, these newly formed dome edges reflow to form lower height domes. SEM images of the key steps in the double-lithography and double-reflow process are shown in figure 3.

The two challenges in the fabrication of multi-height domes are: misalignment of the second exposure step and dome twisting and bubbling resulting from the second development and reflow processes. We next elaborate on these two items.

With respect to the second exposure misalignment, the height of the low profile domes is determined by the width and position of the remaining dome edges, which are UV defined during the second exposure step. Therefore, the alignment accuracy of the second exposure step significantly affects the final height of the low-profile domes, as shown in figure 4. Assuming a pair of low-profile domes formed from a single dome, the height of one dome decreases as the height of the other dome increases during exposure misalignment, which can introduce a large height variation, as shown in figure 5.

In addition to the dome height variation, the peak height position of the dome will shift and present another challenge resulting from misalignment of the second exposure step. Because surface tension dominates the dome profile after reflow, the peak height position of the low-profile dome is always along the center of the remaining dome edge after the second development. If misalignment occurs during the second exposure, the width of the remaining dome edges will change, and so will the center position of the remaining dome edges and the peak position of the low-profile domes after reflow. The shift in the dome peak position becomes very obvious following the fabrication of the MFIs, as shown in figure 6. The height and length of the free-standing portion of the MFIs formed on a dome with a shifted peak height position (figure 6(a)) will be different from those formed using a second exposure step with no misalignment (figure 6(b)). A variation in MFI dimensions will results in an MFI array with non-uniform mechanical and electrical properties, which may present challenges during both assembly and device operation.

The second set of challenges, which consist of dome twisting and bubbling (figure 7), are described next. Dome twisting or delamination following the second photoresist development is caused by poor adhesion between the photoresist dome and the substrate. Using a surface promotor (HDMS, for example) prior to photoresist spin-coating alleviates this issue. Similarly to dome outgassing discussed in [11, 12], dome bubbling is created by insufficient soft-baking of photoresist after the first reflow. Photoresist out gassing becomes more severe as dome height increases.

A multi-height dome array formed using a double-lithography and double-reflow process is shown in figure 8. There are four different zones (I–IV) in the array with each zone corresponding to a specific dome height; the measured height for each of the four zones is shown in figure 9.

The dimensions of the multi-height domes are summarized in table 1. The domes in Zone I are not exposed during the second lithography step and have the largest width (300 μm) and height (66 μm). The domes in Zone II–IV are formed following the second lithography and reflow steps. The second exposure window width defines the width of the exposed area on the original domes, as shown in figure 4, which also determines the width of the removed area from the initial dome. As summarized in table 1, the maximum height difference among the domes formed in this array is 40 μm.

2.2. Fabrication of MPMH MFIs

The fabrication process of the MPMH MFIs is illustrated in figure 2 steps (G)–(L).

The critical step in the fabrication of multi-pitch MFIs is to pattern a photoresist electroplating mold above the multi-height domes. Photoresist spray-coating reported in [13] is adopted here to form a uniform photoresist layer above the

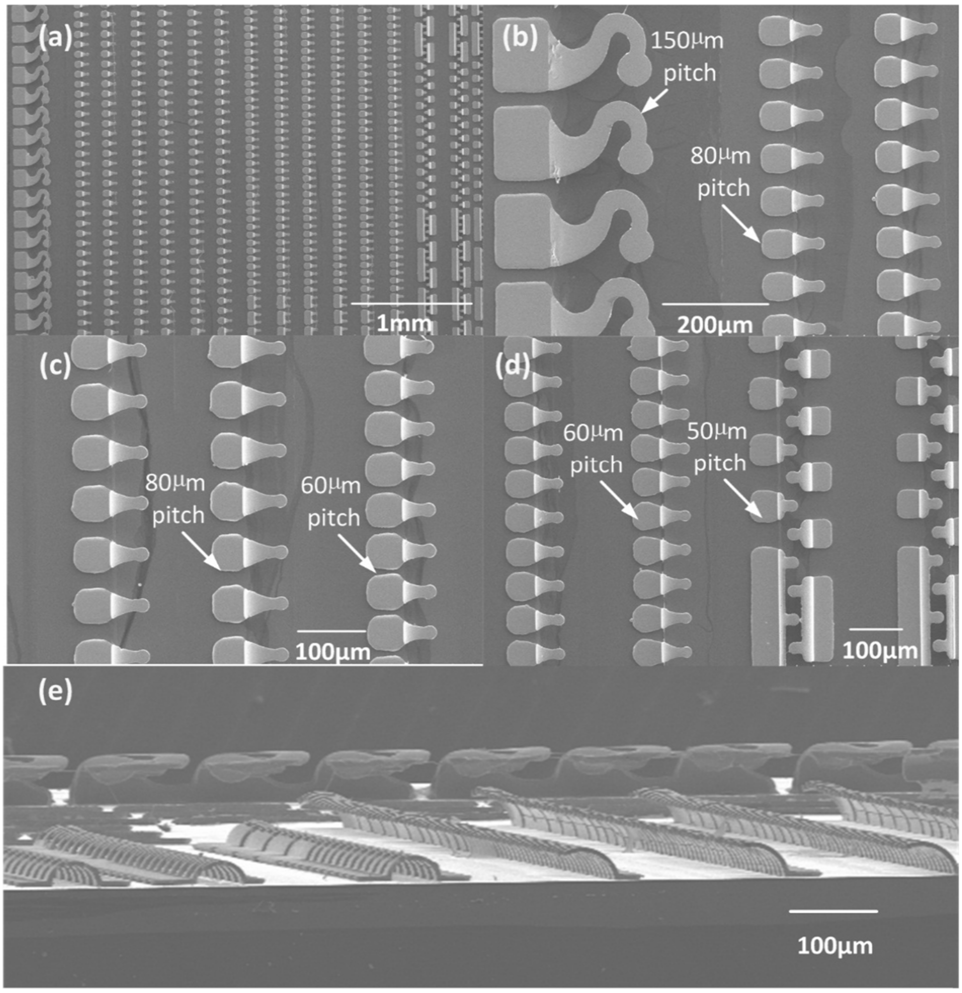

Figure 11. Free-standing MPMH MFI array: (a) top view of the MPMH MFI array, (b–d) detailed view of MFIs with various pitches, and (e) angled view of the MPMH MFI array.

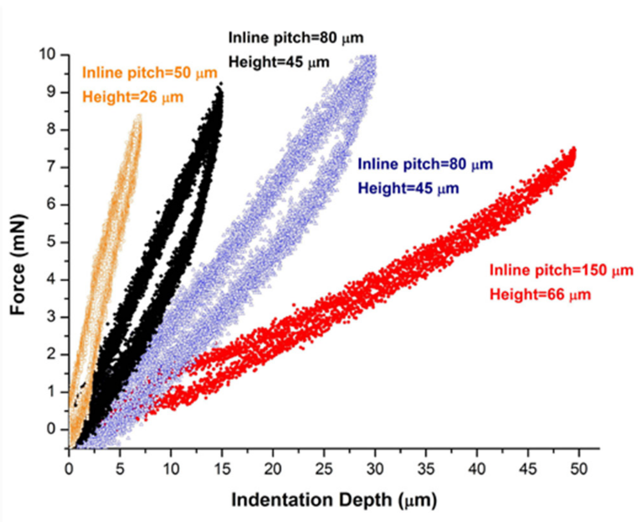

Figure 12. Micro-indentation results of multi-pitch multi-height MFIs.

multi-height domes and circumvent challenges associated to photoresist spin coating. Specifically, spin-coating of the photoresist electroplating mold above the seed layer coated polymer domes yields a non-uniform photoresist layer thickness [12, 13], which introduces two main fabrication challenges: (1) exposure dose control and (2) non-uniform solvent evaporation. On the other hand, the surface profile of the spray-coated photoresist layer perfectly follows the wafer surface topology leading to a uniform photoresist layer thickness. In addition, since most of solvent evaporates during the spray-coating process, low temperature soft bake is sufficient for the subsequent photolithography steps.

Due to the large height variation between the domes (up to 40 μm), the optimization of exposure dose and development time is very challenging and critical to obtain a near perfect exposure over the whole wafer. An electroplating photoresist mold with a large array of multi-pitch MFIs is obtained, as shown in figure 10. The dimensions of the patterns are summarized in table 1. The finest MFI in-line pitch is 50 μm.

Following MFI electroplating, the photoresist electroplating mold, seed layer, and sacrificial domes are removed by photoresist stripper and acid etchant to yield free-standing MPMH MFI array, as shown in figure 11. An overview of the MPMH MFI array is shown in figure 11(a) with more details shown in figures 11(b)–(d). Figure 11(e) shows a prospective view of the MPMH MFIs. Note that this double-lithography and double-reflow process can be used for a number of other applications beyond flexible interconnects.

Table 2. Indentation results.

In-line pitch(μm)	Force (mN)	Indentation depth (μm)	Measured compliance (mm N^{-1})	Simulated compliance (mm N^{-1})
150	7.5	50	6.67	6.52
80	9.6	30	3.12	2.88
60	9.3	15	1.61	1.47
50	8.5	7	0.82	0.73

Table 3. Four point resistance measurement.

In-line pitch (μm)	Resistance (mΩ)	Standard deviation (mΩ)	Simulated resistance (mΩ)
150	128.6	2.6	122.2
80	69.5	3.4	63.5
60	54.3	3.7	50.5
50	37.6	4.1	34.6

3. Results and discussion

Mechanical indentation and electrical characterization of the MPMH MFIs are described in this section.

3.1. Mechanical indentation test

Indentation tests are performed using the same procedures discussed in [9–11]. Figure 12 and table 3 summarize the results of micro-indentation. As shown in table 3, the compliance of MFIs on a 50 μm pitch is smaller than MFIs on a 150 μm pitch, which is due to the difference in effective length.

3.2. Electrical resistance test

The electrical characterization of the MPMH MFIs is performed using a four-point resistance measurement as described in [10, 11]. The measured results and simulated results are summarized in table 3 and demonstrate high yield. During the measurements, the tested MFIs are partially bent to attain a stable resistance reading.

4. Conclusions

This paper reports a double-lithography and double-reflow process for the fabrication of multi gap-height MEMS structures. Low-cost wafer-level batch fabricated MPMH MFIs are reported in this paper. The height variation of the demonstrated MPMH MFIs is up to 40 μm for a pitch range of 150 μm–50 μm. Mechanical micro-indentation testing and four-point resistance measurements of the MPMH MFIs are performed for initial mechanical and electrical characterization.

References

[1] Bakir M *et al* 2003 SoL ultra high density wafer level chip input/output interconnections for gigascale integration (GSI) *IEEE Trans. Electron. Devices* **50** 2039–48

[2] Shubin I *et al* 2009 Novel packaging with rematable spring interconnect chips for MCM *59th Electronic Components and Technology Conf. (San Diego, California)* pp 1053–8

[3] Ma L, Zhu Q, Hantschel T, Fork D K and Sitaraman S K 2002 J-springs—innovative compliant interconnects for next-generation packaging *57th Electronic Components and Technology Conf. (Reno, Nevada)* pp 1359–65

[4] Kacker K, Sokol T and Sitaraman S K 2007 Flex connects: a cost-effective implementation of compliant chip-to-substrate interconnects *Proc. 57th Electronic Components and Technology Conf. (Reno, Nevada)* pp 1678–84

[5] Spanier G *et al* 2007 Platform for temporary testing of hybrid microsystems at high frequencies *J. MEMS* **16** 1367–77

[6] Choe S-H, Tanaka S and Esashi M 2007 MEMS-based probe array for wafer level LSI testing transferred onto low CTE LTCC substrate by Au/Sn eutectic bonding *TRANSDUCERS 2007—Int. Solid-State Sensors, Actuators and Microsystems Conf. (Lyon, 10–14 June 2007)* pp 2517–20

[7] Tsunoda T *et al* 2014 Advanced vertical interconnect technology with high density interconnect and conductive paste *2014 Int. Conf. Electronics Packaging (ICEP) (Toyama, 23–25 April 2014)* pp 50–4

[8] Sutanto J *et al* 2013 Development of chip-on-chip with face to face technology as a low cost alternative for 3D packaging *2013 IEEE 63rd Electronic Components and Technology Conf. (Las Vegas, Nevada)* pp 955–65

[9] Yang H S and Bakir M S 2012 Design, fabrication, and characterization of freestanding mechanically flexible interconnects using curved sacrificial layer *IEEE Trans. Compon. Packag. Manuf. Technol.* **2** 561–8

[10] Zhang C, Yang H S and Bakir M S 2012 Gold passivated mechanically flexible interconnects (MFIs) with high elastic deformation *2012 IEEE 62nd Electronic Components and Technology Conference (San Diego, California, May 2012)* pp 245–50

[11] Zhang C, Yang H S and Bakir M S 2013 Highly elastic gold passivated mechanically flexible interconnects *IEEE Trans. Compon. Packag. Manuf. Technol.* **3** 1632–9

[12] Zhang C, Yang H S and Bakir M S 2014 Mechanically flexible interconnects with highly scalable pitch and large stand-off height for silicon interposer tile and bridge interconnection *2014 IEEE 64th Electronic Components and Technology Conference (ECTC) (Orlando, FL, May 2014)* pp 13–9

[13] Zhang C *et al* 2014 Mechanically flexible interconnects (MFIs) with highly scalable pitch *J. Micromech. Microeng.* **24** 055024

[14] Namburi L *et al* 2013 A fine pitch MEMS probe card with built in active device for 3D IC test *IEEE SW Test Workshop (June 2013)*

[15] Yang H S *et al* 2014 Self-aligned silicon interposer tiles and silicon bridges using positive self-alignment structures and rematable mechanically flexible interconnects *IEEE Trans. Compon. Packag. Manuf. Technol.* **4** 1760–8

[16] Zhang C, Thadesar P, Zia M, Sarvey T and Bakir M S 2014 Au-NiW mechanically flexible interconnects (MFIs) and TSV integration for 3D interconnects *2014 Int. 3D Systems Integration Conf. (3DIC) (Kinsale, 2014)* pp 1–4

[17] Yang H S, Zhang C, Zia M, Zheng L and Bakir M S 2014 Interposer-to-interposer electrical and silicon photonic interconnection platform using silicon bridge *2014 Optical Interconnects Conf. (San Diego, CA, 2014)* pp 71–2

[18] Zhang Y *et al* 2016 Thermal isolation using air gap and mechanically flexible interconnects for heterogeneous 3D ICs *IEEE Trans. Compon. Packag. Manuf. Technol.* **6** 31–9